Published in final edited form as:
Cell Metab. 2014 August 5; 20(2): 267–279. doi:10.1016/j.cmet.2014.05.003.

Lipin-1 Regulates Autophagy Clearance and Intersects with Statin Drug Effects in Skeletal Muscle

Peixiang Zhang[1], **M. Anthony Verity**[2], and **Karen Reue**[1,3,4]

[1]Department of Human Genetics, David Geffen School of Medicine at UCLA, Los Angeles, CA 90095 USA

[2]Division of Neuropathology, Department of Pathology and Laboratory Medicine, David Geffen School of Medicine at UCLA, Los Angeles, CA 90095 USA

[3]Department of Medicine, David Geffen School of Medicine at UCLA, Los Angeles, CA 90095 USA

[4]Molecular Biology Institute, University of California, Los Angeles, CA 90095 USA

SUMMARY

LPIN1 encodes lipin-1, a phosphatidic acid phosphatase (PAP) enzyme that catalyzes the dephosphorylation of phosphatidic acid to form diacylglycerol. Homozygous *LPIN1* gene mutations cause severe rhabdomyolysis, and heterozygous *LPIN1* missense mutations may promote statin-induced myopathy. We demonstrate that lipin-1–related myopathy in the mouse is associated with a blockade in autophagic flux and accumulation of aberrant mitochondria. Lipin-1 PAP activity is required for maturation of autolysosomes, through its activation of the protein kinase D (PKD)-Vps34 phosphatidylinositol 3-kinase signaling cascade. Statin treatment also reduces PKD activation and autophagic flux, which are compounded by diminished mTOR abundance in lipin-1-haploinsufficent and –deficient muscle. Lipin-1 restoration in skeletal muscle prevents myonecrosis and statin toxicity *in vivo*, and activated protein kinase D rescues autophagic flux and lipid homeostasis in lipin-1–deficient cells. Our findings identify lipin-1 PAP activity as a component of the macroautophagy pathway, and define the basis for lipin-1–related myopathies.

INTRODUCTION

Lipin-1 is a phosphatidic acid phosphatase (PAP) enzyme, which converts phosphatidic acid (PA) to diacylglycerol (DAG), a precursor of triacylglycerol and phospholipids (Donkor et al., 2007; Han et al., 2006). Lipin-1 is also a co-regulator of DNA-bound transcription factors (Finck et al., 2006; Kim et al., 2010; Peterson et al., 2011; Sugden et al., 2010), which in some cases requires its PAP activity (Peterson et al., 2011). Lipin-1 is a target of

Correspondence to: Karen Reue, David Geffen School of Medicine at UCLA, Department of Human Genetics, Gonda 6506A, 695 Charles E. Young Drive South, Los Angeles, CA 90095. Tel 310-794-5631; Fax 310-794-5446; reuek@ucla.edu.

the mechanistic target of rapamycin complex 1 (mTORC1), and lipin-1 subcellular localization and function are regulated by mTORC1-dependent phosphorylation at multiple sites (Eaton et al., 2013; Harris et al., 2007; Huffman et al., 2002; Peterson et al., 2011). Through these activities, lipin-1 and its orthologs in diverse species regulate adipogenesis, lipid metabolism, nuclear envelope and mitochondrial morphology, and vacuole fusion (Csaki et al., 2013; Pascual and Carman, 2013).

Recently, recessive *LPIN1* gene mutations have been identified as a cause of childhood rhabdomyolysis (Bergounioux et al., 2012; Michot et al., 2010; Michot et al., 2012; Zeharia et al., 2008). Rhabdomyolysis, a severe form of myopathy, is characterized by breakdown of skeletal muscle resulting in leakage of muscle-cell contents such as electrolytes, creatine kinase, and myoglobin, into the circulation. Episodes of *LPIN1*-related rhabdomyolysis appear to be precipitated by febrile illness, exercise, fasting, or anesthesia (Bergounioux et al., 2012; Zeharia et al., 2008). Nearly all *LPIN1* mutations that cause childhood rhabdomyolysis are nonsense or deletion mutations, which are predicted to result in inactive protein (Michot et al., 2010; Michot et al., 2012; Zeharia et al., 2008). Myopathy has also been reported in individuals that are heterozygous for *LPIN1* missense mutations in response to statin drug treatment (Michot et al., 2012; Zeharia et al., 2008). Statins are widely prescribed cholesterol-lowering drugs that reduce the incidence of cardiovascular diseases. An estimated 1-5% of statin drug users complain of muscle symptoms, and a small proportion develop rhabdomyolysis (Mohassel and Ammane, 2013; Thompson et al., 2003). The underlying mechanisms for statin myotoxicity are not understood, but there is evidence that underlying genetic variations may predispose some individuals (Link et al., 2008; Mangravite et al., 2013; Needham and Mastaglia, 2013). Relevant to the pathology of *LPIN1*- related myopathies, lipin-1 accounts for the majority of PAP activity in human and mouse skeletal muscle (Donkor et al., 2007; Harris et al., 2007; Michot et al., 2013), and the transgenic modulation of muscle lipin-1 levels alters energy balance (Phan and Reue, 2005). Human lipin-1–deficient muscle and myoblasts accumulate neutral lipid droplets (Michot et al., 2012; Michot et al., 2013), but it is unclear how this relates to the massive muscle breakdown in affected patients.

We sought to elucidate the mechanism underlying myopathy in both lipin-1 deficiency and in response to statin treatment in the presence of reduced lipin-1 activity. We identified a role for lipin-1 in autophagy, and determined that lipin-1 deficiency and statin drug effects converge at specific points of lipid metabolism that influence autophagic flux.

RESULTS

Myonecrosis in Lipin-1–deficient and Statin-treated Lipin-1–haploinsufficient Mice

To investigate the pathoetiology of inherited and statin-induced lipin-1-related myopathies, we utilized mouse models with lipin-1 deficiency (*Lpin1*$^{fld/fld}$ mice (Peterfy et al., 2001), denoted "*fld/fld*") or with half the normal lipin-1 levels (*Lpin1*$^{wt/fld}$ mice, denoted "*wt/fld*") (Figure 1A). *LPIN1*-related rhabdomyolytic episodes are associated with metabolic stress, including fasting. We found that muscle damage is triggered in *fld/fld* mice by fasting for 16 hr followed by 5 hr refeeding. These conditions elevated creatine kinase (CK) levels, and were employed throughout our studies. The CK levels in *fld/fld* mice were exacerbated by

treatment with Pravastatin (375 μg/day/mouse in the drinking water for 11 weeks) (Figure 1B). Heterozygous (*wt/fld*) mice had normal CK levels under basal conditions, but increased above wild-type levels following statin treatment (Figure 1B).

Myofibrillar necrosis was evident in *fld/fld* mice, and was enhanced by statin treatment (Figure 1C). Muscle from *fld/fld* mice also exhibited centrally located myonuclei, indicative of regenerating fibers (Chargé and Rudnicki, 2004), which became more prevalent upon statin treatment (Figure 1D). Centrally nucleated fibers were not observed in *wt/fld* muscle under the basal conditions, but became apparent after statin treatment (Figure 1D). Thus, lipin-1–deficient muscle exhibits necrosis and regeneration, and statin treatment promotes muscle damage in lipin-1–haploinsufficient mice and lipin-1–deficient mice.

Since lipin-1 catalyzes a step in triacylglycerol (TAG) biosynthesis, we expected that *fld/fld* muscle would have reduced neutral lipid storage. Staining of muscle with oil red O revealed an unexpected accumulation of neutral lipid droplets in lipin-1–deficient muscle, primarily in type I fibers (Figures 1E and S1A). This pattern of lipid accumulation is similar to that reported in a *LPIN1*-deficient patient (Michot et al., 2012), and in a subset of human statin-intolerant myopathy patients (Phillips et al., 2002); the identity of neutral lipid accumulating in these patients has not been determined. Biochemical analyses revealed that *fld/fld* muscle contained very little TAG, and that *wt/fld* muscle contained approximately 50% of wild-type levels (Figure 1F). By contrast, cholesteryl ester levels were elevated by 2-fold in *fld/fld* muscle under the basal condition, and were elevated further after statin treatment (Figure 1F). Cholesteryl ester accumulation likely accounts for the neutral lipid droplets observed in lipin-1–deficient muscle. Free fatty acid levels were also elevated in *fld/fld* muscle in basal and statin-treated conditions, and in *wt/fld* muscle after statin treatment (Figure 1F). We did not detect increased expression of fatty acid synthetic genes in *fld/fld* muscle (Figure S1B), and it is possible that fatty acids accumulating in muscle are derived from other tissues. Given the role of lipin-1 in coactivation of hepatic fatty acid oxidation genes (Finck et al., 2006), we examined expression of known target genes (*Cpt1b*, *Acadm*, *Acadl*, *Acox1*) in muscle. Gene expression levels were similar in *fld/fld* and wild-type muscle (Figure S1C), suggesting that fatty acid accumulation is not a result of impaired lipin-1 coactivator function.

Analysis of phospholipid and sphingolipid content by electrospray ionization mass spectrometry revealed substantial alterations in lipin-1–deficient muscle. PA, the substrate for lipin-1 enzymatic activity, was elevated 3-fold in *fld/fld* muscle (Figure 1F and S1D). In addition, *fld/fld* muscle had elevated levels of ether phosphatidylcholine (ePC) and ceramides (Figure S1D). Thus, the accumulation of several aberrant lipid species (cholesteryl ester, fatty acids, and various phospholipids, and ceramides) may contribute to altered metabolism in lipin-1–deficient muscle.

Muscle Lipin-1 Rescues Basal and Statin-induced Myonecrosis in Lipin-1–deficient Mice

To determine whether the loss of lipin-1 locally in skeletal muscle is responsible for myonecrosis observed in *fld/fld* mice, we rescued lipin-1 expression with a muscle-specific lipin-1 transgene (Phan and Reue, 2005). By crossing the Mck-lipin-1 transgene into *fld/fld* mice, we generated animals with lipin-1 exclusively in skeletal muscle (referred to as *fld/*

fld–MCK Tg; Figure 2A). Transgenic restoration of lipin-1 in muscle of *fld/fld* mice prevented muscle damage, as indicated by normalized CK levels and reduced myocyte turnover (Figures 2B and 2C), and largely normalized the reduced myofiber size that occurs in *fld/fld* soleus and tibialis anterior muscle (Figure S2A). The restoration of lipin-1 *fld/fld* muscle prevented the accumulation of neutral lipids in type 1 fibers (Figure 2D and S2B), increased TAG levels, and normalized cholesteryl ester, fatty acids, PA, ePC and ceramide levels (Figures 2E-H and S2C). Furthermore, lipin-1 expression in muscle protected against the statin-associated muscle damage in both *wt/fld* and *fld/fld* mice (Figures 2B, 2C and S2D).

Lipin-1 Deficiency Impairs Mitochondrial Function and Autophagy in Muscle

The aberrant lipid profile in type I muscle fibers of lipin-1–deficient muscle led us to investigate mitochondrial activity. We examined mitochondrial ultrastructure in *fld/fld* muscle by transmission electron microscopy (EM). The *fld/fld* soleus muscle exhibited large, misshapen mitochondria. After statin treatment, disorganized cristae were also evident (Figure 3A and S3A). By contrast, mitochondria of wild-type muscle had normal morphology, even after statin treatment. Increased mitochondrial number was also evident in *fld/fld* muscle, as judged by the increased levels of mitochondrial DNA relative to genomic DNA (Figure 3B). To assess mitochondrial function, we measured oxygen consumption in soleus muscle from wild-type and *fld/fld* mice. Basal oxygen consumption rates did not differ, but when challenged with a mitochondrial uncoupler, wild-type muscle responded with the expected increase in oxygen consumption, whereas the response in *fld/fld* muscle was severely blunted (Figure 3C).

Mitochondrial quality is tightly controlled by autophagy, a process by which damaged mitochondria are degraded (Wang and Klionsky, 2011). A knockdown in the expression of the lipin ortholog in *Drosophila* (Dlipin) leads to an accumulation of abnormal mitochondria and autophagosomes in the fat body (Ugrankar et al., 2011). We hypothesized that damaged mitochondria might accumulate in lipin-1–deficient muscle because of impaired autophagy. Autophagy is induced under starvation and other conditions and begins with the formation of a limiting membrane that encompasses cytosolic proteins and organelles by forming a vesicular autophagosome; the autophagosome then fuses with a lysosome to produce an autolysosome, and degrades its contents (Wang and Klionsky, 2011). We assessed the induction of autophagy by examining the levels of the autophagosome marker, microtubule-associated protein-1 light chain 3 (LC3)-II (Kabeya et al., 2000).

In wild-type muscle, fasting led to the expected induction of LC3-II, which was not apparent after feeding (Figure 3D, *upper panel*). Muscle from *fld/fld* mice induced autophagosome formation in response to fasting, but maintained high levels of LC3-II even after refeeding; statin treatment further elevated the levels of LC3-II in *fld/fld* mice (Figure 3D, *lower panel*). We also estimated autophagic flux by quantitating the levels of p62, an autophagy-selective substrate (Mizushima et al., 2010). Compared to wild-type muscle, *fld/fld* muscle accumulated twice as much p62 (Figure 3D and S3B). Interestingly, statin treatment caused a modest increase in p62 protein levels in wild-type muscle, albeit less than that observed in lipin-1–deficient muscle (Figure S3B). Neither lipin-1 deficiency nor statin treatment

influenced p62 mRNA expression levels, consistent with effects on p62 clearance, rather than synthesis (Figure S3B). The LC3-II and p62 levels in *fld/fld* muscle were restored to wild-type levels by expression of the muscle-specific lipin-1 transgene (Figure 3E). These studies demonstrate that lipin-1 is dispensable for the formation of autophagosomes, but is required for clearance of autolysosome cargo (*e.g.*, LC3-II and p62).

To learn more about the role of lipin-1 in autophagy, we assessed the localization of lipin-1 by co-staining C2C12 myotubes with antibodies against endogenous lipin-1 and LAMP-1, a lysosomal protein that has a role in the fusion of lysosomes with phagosomes (Huynh et al., 2007). Under basal conditions, lipin-1 protein had a diffuse cytoplasmic distribution (Figure 3F, *left panels*). Treatment with rapamycin, which inhibits mTOR and induces autophagy, promoted migration of lipin-1 to the perinuclear region and partial co-localization with Lamp1 (Figure 3F, *middle panels*). Statin treatment promoted a similar reorganization of lipin-1 to that observed with rapamycin treatment (Figure 3F, *right panels*). Thus, both the induction of autophagy and statin treatment promote lipin-1 co-localization with lysosomes. To exclude the possibility that lipin-1 co-localizes with lysosomes affects lipin-1 protein stability, we treated cells expressing lipin-1 with inhibitors of lysosomal (chloroquine) or proteasomal degradation (MG-132). We found that only MG-132 inhibited lipin-1 protein degradation (Figure 3G). This is consistent with findings for the lipin ortholog in yeast (Pascual et al., 2014).

Lipin-1 PAP Activity is Required for Autophagy Clearance

We next examined whether the PAP activity of lipin-1 was required for autophagy using a reporter consisting of LC3 conjugated to a red fluorescent protein (RFP) and a green fluorescent protein (GFP) (RFP-GFP-LC3) (Kimura et al., 2007). This reporter distinguishes autophagosomes (yellow signal, due to fluorescence from both RFP and GFP) from autolysosomes (red signal, due to RFP alone, as GFP fluorescence is impaired in the acidic lysosomal environment). In wild-type mouse embryonic fibroblasts (WT-MEFs), the induction of autophagy by serum and amino acid starvation induced the formation of autolysosomes (red puncta), indicating progression through the autophagy pathway (Figure 4A). Starvation-induced autolysosome formation was reduced by 50% in lipin-1–deficient MEFs (*fld*-MEF) (Figures 4A and 4B). The blockade in autolysosome formation in *fld*-MEFs was rescued by overexpression of wild-type, but not catalytically inactive, lipin-1 (Figure 4A, left and top right panel). These results were confirmed by analysis of LC3-II protein levels (Figure S4A). Rapamycin induced similar levels of LC3-II in WT-MEFs and *fld*-MEFs, demonstrating that formation of autophagosomes is not impaired by lipin-1 deficiency. However, *fld*-MEFs exhibited impaired clearance of LC3-II in response to serum starvation, which could be rescued by wild-type but not mutant lipin-1 expression (Figure S4A). The requirement of lipin-1 PAP activity in autophagy was further confirmed by the analysis of PA and DAG levels in these primary MEFs. Compared to wild-type cells, lipin-1–deficient MEFs contained higher PA and lower DAG levels after 6h starvation; overexpression of wild-type, but not PAP-deficient lipin-1 protein restored these lipid levels (Figure 4A, *right panel*).

To further explore the role of lipin-1 in autophagy clearance, the fusion of autophagosomes with lysosomes was examined in primary WT-MEFs and *fld*-MEFs. Starvation induced the fusion of autophagosomes with lysosomes or late endosomes in wild-type cells, as indicated by the perinuclear co-localization of LC3 and LAMP-1 (Fig. 4B). By contrast, lipin-1 deficiency prevented perinuclear clustering of lysosomes upon starvation, and reduced fusion between autophagosomes and lysosomes or late endosomes (Figure 4B and S4B). The degree of LC3-LAMP-1 co-localization observed in wild-type MEFs is similar to that shown in previous studies that visualize autophagosome-lysosome fusion by this method (Germain et al., 2011; Liang et al., 2008).

Lipin-1 Deficiency Diminishes DAG–Protein Kinase D–Vps34 Activation in Muscle

The requirement for lipin-1 PAP activity in autophagy clearance raised the possibility that lipin-1 conversion of PA to DAG is important in this process. Indeed, it has been shown that DAG is required for clearance of bacteria by autophagy in mammalian cells (Shahnazari et al., 2010). The role of DAG in this process is likely linked to its function as a lipid second messenger. DAG activates a signaling cascade involving protein kinase C, with subsequent activation of the class III phosphatidylinositol 3-kinase, Vps34, which is involved in autophagosome formation and maturation (Eisenberg-Lerner and Kimchi, 2012; Shibasaki et al., 2009; Tan et al., 2012). We hypothesized that lipin-1–generated DAG is important in autolysosome formation, and that lack of lipin-1 impairs PKC and Vps34 activation. Below we describe studies to test each component of this hypothesis.

Using electrospray ionization mass spectrometry, we identified several DAG species with reduced levels in *fld/fld* muscle (Figure 5A). To assess whether the reduced DAG levels influence autophagy clearance, we reconstituted *fld*-MEFs with dipalmitoylglycerol (C32:0), the most abundant of the DAG species that showed reduced levels in *fld/fld* muscle. The addition of dipalmitoylglycerol to *fld*-MEFs did not affect autophagosome formation in the early phase of starvation-induced autophagy (Figure S5A), but restored autophagy clearance by reduction of the levels of LC3-II (Figure 5B).

We next assessed whether the altered DAG profile of *fld/fld* muscle led to impaired PKC activation. The mammalian PKC family consists of approximately a dozen isoforms, several of which are expressed in skeletal muscle (Ellwanger et al., 2011; Jensen et al., 2009). We analyzed the activation of relevant PKC isoforms by western blot using antibodies directed against the phosphorylated proteins. Most PKC isoforms in muscle showed similar levels of phosphorylation (activation) in wild-type and *fld/fld* muscle (Figure 5C). The exception was phosphorylated PKD, which was substantially reduced in *fld/fld* muscle, despite normal levels of total PKD (Figure 5C). The muscle lipin-1 transgene largely restored PKD activation in the muscle of *fld/fld* mice (Figure 5D). Statin treatment also markedly diminished PKD activation in wild-type muscle (Figure 5E), revealing a common effect of lipin-1 deficiency and statin drug response.

PKD activates Vps34 leading to the production of phosphatidylinositol-3-phosphate (PtIns3P) (Eisenberg-Lerner and Kimchi, 2012), and Vps34-derived PtIns3P has an established role in the promotion of autophagosome formation and maturation (Jaber et al., 2012). Because PKD activation was diminished in *fld/fld* muscle (Figure 5C), we sought to

determine whether Vps34 activity was affected by assessing the formation of PtIns3P. We used a green fluorescent reporter containing the PtIns3P-binding PX-domain (phox) from p40 (GFP- p40 ^{phox}) (Kanai et al., 2001). When co-expressed with a reporter containing the autophagosome/autolysosome marker LC3 fused to red fluorescent protein (mRFP-LC3), it was possible to visualize PtIns3P present on autophagosome/autolysosome structures as yellow puncta. Serum starvation to induce autophagy led to the appearance of many more yellow puncta in WT-MEFs (Figure 5F, *upper panels*) than *fld*-MEFs (Figure 5F, *lower panels*). Quantitation revealed approximately 50% reduction in PtIns3P in *fld*/*fld* compared to wild-type cells, consistent with reduced Vps34 activity.

A prediction from the findings described above is that activated PKD should rescue autophagy flux observed in lipin-1–deficient cells. To test this, we co-expressed constitutively active PKD (S738E/742E) (Storz et al., 2003) with the RFP-GFP-LC3 reporter (Kimura et al., 2007) in *fld*-MEFs. The expression of active PKD rescued autolysosome formation in *fld*-MEFs to nearly the level observed in WT-MEFs (Figures 5G). These results indicate that lipin-1/DAG signaling is a critical component of the PKD-Vps34 signaling cascade, and that disruption of this cascade is a likely cause of apparently impaired autophagy flux in lipin-1–deficient muscle.

Statin Diminishes mTOR Protein Abundance and Promotes Abnormal Lipid Accumulation in Combination with Lipin-1 Haploinsufficiency

We next investigated the mechanisms underlying statin-induced myopathy in lipin-1-haploinsufficient mice and statin-exacerbated myopathy in lipin-1-deficient mice. Although statins have been shown to induce FoxO3/atrogin-1-mediated muscle cell damage (Hanai et al., 2007), 11-weeks of Pravastatin treatment did not alter the activation of Akt/FoxO3 in wild-type or *fld/fld* muscle (Figure 6A). However, statin treatment led to substantially diminished levels of mammalian target of rapamycin (mTOR) in *fld/fld* muscle. Both total and phosphorylated mTOR (p-mTOR) were reduced, and mTOR activity was decreased as indicated by diminished phosphorylation of the mTOR target, p70-S6 kinase (on Thr389) (Figure 6A). The levels of regulatory associated protein of mTOR (Raptor) were not affected by lipin-1 deficiency or statin treatment (Figure 6A). Statin treatment also reduced mTOR abundance in lipin-1-haploinsufficient muscle (Figure 6B), and the muscle lipin-1 transgene largely restored the levels of mTOR protein in the muscle of *fld/fld* mice under statin treatment (Figure 6C).

Finally, we examined whether statin treatment influenced muscle lipid content in a manner that compounds the effects of lipin-1 haploinsufficiency. Statin treatment increased PA levels in wild-type muscle and lipin-1-haploinsufficient muscle to levels that were similar to those accumulating in response to PAP enzyme deficiency in *fld/fld* muscle (Figure 6D). Acute statin treatment in C2C12 myotubes increased PA levels by about 25% (Fig. S6). Statin also promoted accumulation of ceramide, ether phosphatidylcholine, phosphatidylcholine, and sphingomyelin in lipin-1–hapoinsufficient and lipin-1–deficient muscle (Figure 6E-F). Thus, statin treatment exacerbates lipid imbalances in lipin-1–deficient muscle, and induces similar lipid abnormalities in lipin-1–haploinsufficient muscle. Together, reduced lipin-1 levels and statin treatment intersect to induce autophagy (due to

reduced mTOR), but also reduce the capacity for autophagy flux (due to increased PA and reduced PKD activation), leading to impaired autophagy clearance (Figure 7).

DISCUSSION

The pathogenic mechanism for *LPIN1*-related myopathy is unknown. Here, we describe an essential role for lipin-1 in maintenance of muscle integrity through autophagy. Lipin-1 PAP activity is required for the generation of DAG and activation of the PKD-Vps34 signaling cascade in autophagy clearance (Figure 7, *left panel*). In the case of lipin-1 deficiency, a blockade in PAP activity leads to reduced DAG levels and impaired activation of PKD–Vps34, preventing normal maturation of autolysosomes (Figure 7, *right panel* red arrows). These defects likely contribute to rhabdomyolysis observed in lipin-1 deficiency. We uncovered intersecting actions of lipin-1 and statin drugs on components of this pathway. Like lipin-1 deficiency, statin treatment caused PA accumulation and reduced PKD activation, even in wild-type mice (Figure 7, *right panel* blue arrows). Additionally, statin treatment of lipin-1–deficient and – haploinsufficient mice led to reduced mTOR activity, which is a trigger for autophagy induction. The combination of enhanced autophagy initiation and impaired capacity for flux through the pathway induced statin-related myopathy in mice with reduced lipin-1 activity.

We determined that lipin-1 PAP activity is critical for both activation of the PKD-Vps34 pathway and for TAG synthesis and storage in muscle. Previous studies showed that DAG formation by PAP activity is important for activation of PKD in Golgi vesicle trafficking, but it was unclear whether one of the lipin PAP enzymes or the lipid phosphate phosphatases (previously known as PAP2 enzymes) are responsible (Asp et al., 2009; Baron and Malhotra, 2002; Fernandez-Ulibarri et al., 2007). Here we demonstrate that lipin-1 PAP activity is required for PKD activation and fusion of autophagosomes to lysosomes. The addition of exogenous dipalmitoylglycerol, or expression of constitutively active PKD, both largely rescued autophagy flux in lipin-1–deficient cells. This defines a previously unknown role for lipin-1 enzyme activity in macroautophagy. Furthermore, it suggests that PKD activation could be a potential therapeutic approach for treatment of lipin-1–related rhabdomyolysis.

Our results also demonstrate that lipin-1 controls TAG storage in muscle. We previously showed that lipin-1 transgene expression in muscle of wild-type mice leads to obesity and insulin resistance, which may be influenced, in part, by enhanced TAG accumulation in muscle (Phan and Reue, 2005). The current study highlights the detrimental effects of lipin-1 deficiency on lipid homeostasis in muscle. Failure to synthesize and store TAG led to an accumulation of unesterified fatty acids. A recent study demonstrated that myocytes isolated from lipin-1–deficient patients also accumulate fatty acids, and suggested that increased fatty acid synthesis may contribute (Michot et al., 2013). We did not observe evidence for increased fatty acid synthesis, but did observe increased neutral lipid content in the form of cholesteryl ester; we suspect that cholesteryl ester also accounts for the neutral lipid droplets appearing in human lipin-1–deficient muscle. Cholesteryl esters may accumulate as an alternative pathway to neutralize excess fatty acids in the absence of TAG synthesis. It is also possible that the accumulation of fatty acids, phospholipids, and

ceramides in lipin-1–deficient muscle contributes to the impaired autophagy and/or mitochondrial function observed (Las et al., 2011).

Autophagy has an important housekeeping role in the routine clearance of protein aggregates and damaged organelles, and the accumulation of abnormal mitochondria in lipin-1–deficient muscle may result from impaired autophagic flux. Autophagy can also serve to non-selectively degrade cytosolic contents to supply cells with essential macromolecules and energy, and to ensure cellular survival during starvation (Levine and Kroemer, 2008). A mysterious aspect of human lipin-1 deficiency is that patients exhibit normal muscle function between rhabdomyolytic episodes, suggesting that mitochondrial function is adequate to meet energy demands during everyday activities. The rhabdomyolitic episodes are typically associated with fasting or intense exercise. Since fasting and exercise also trigger autophagy (He et al., 2012), it is possible that the demand for autophagy during these stresses provides the basis for induction of muscle damage in lipin-1–deficient individuals under specific circumstances.

The observation that heterozygous *LPIN1* mutation can be associated with statin-induced myopathy inspired us to investigate the potential convergence of lipin-1 function and statin toxicity. We determined that a 50% reduction of *Lpin1* expression in mouse, similar to what may occur in the heterozygous carriers of inactivating *LPIN1* mutations, promotes muscle damage in a statin-dependent manner. In our model, statins impaired intramuscular lipid homeostasis, as indicated by the accumulation of FFA, PA, ether phospholipids and ceramides. Interestingly, statin treatment *in vivo* produced two alterations that were also observed as a consequence of lipin-1 deficiency—increased PA levels and reduced PKD activation—and these effects occurred even in wild-type mice. PA levels were also increased by treatment with three different statins in C2C12 myocytes. These observations raise the question of whether statins act to inhibit lipin-1. We determined that statin treatment does not reduce *Lpin1* mRNA levels in mouse muscle. However, it remains possible that statins increase PA levels through altering lipin-1 protein localization or stabilization, or through lipin-1–independent processes, such as activation of diacylglycerol kinase or phospholipase D. Along these lines, lovastatin enhances the catalytic activity of phospholipase D2, promoting PA production (Cho et al., 2011).

Statin treatment in combination with lipin-1-haploinsufficiency or lipin-1-deficiency produced more severe aberrations in cellular lipid homeostasis that with either perturbation alone, with increased levels of several phospholipids and sphingomyelin. Together, impaired lipin-1 levels and statin treatment also led to reduced mTOR and phospho-mTOR abundance. It has been demonstrated that persistent inactivation of mTORC1 blocks autophagy clearance and induces myopathy (Ching et al., 2013; Yu et al., 2010). Thus, the combined effect of statin treatment and reduced lipin-1 content in heterozygous mice may account for the similar (although less severe) phenotype as that observed in lipin-1–deficient mice. It should be noted that the majority of muscle symptoms reported by individuals taking statin drugs are not accompanied by biochemical or pathological evidence of muscle disease, and the adverse muscle effects described here are most relevant to the rare cases of statin-induced rhabdomyolysis. Our data suggest that heterozygous carriers of *LPIN1*

mutations, which have been detected in the general population (http://www.1000genomes.org/data), may be at risk for statin-induced rhabdomyolysis.

In summary, we demonstrate that lipin-1 PAP activity functions in autophagy to activate the PKD–Vps34 cascade to promote autolysosome maturation. The loss of lipin-1 activity leads to an accumulation of aberrant mitochondria and lipids in skeletal muscle. Statin treatment also impairs PKD activation, which is compounded by lipin-1 deficiency or haploinsufficiency. The demonstration that lipin-1 is required for autophagy clearance suggests novel therapeutic approaches for lipin-1– and statin-related rhabdomyolysis.

EXPERIMENTAL PROCEDURES

Animals

BALB/cByJ *Lpin1*$^{wt/fld}$ mice were obtained from the Jackson Laboratory (Bar Harbor, ME) and bred to generate mice of desired genotypes. We generated mice with lipin-1 expression exclusively in muscle by crossing a MCK (muscle creatine kinase)-lipin-1 transgene onto the *Lpin1*$^{fld/fld}$ background as we did previously (Phan and Reue, 2005). For statin treatment, Pravastatin (150 μg/ml) was administered to female mice (aged 2-3 months) in the drinking water, with an average consumption of 2.5 ml/day/mouse for 11 weeks. In pilot experiments, circulating creatine kinase levels were elevated in *fld/fld* mice most significantly in a refed state, and mice were therefore fasted 16 h and refed for 5 h (0800-1300) before blood and tissue collection. The institutional Animal Care and Use Committee of the University of California Los Angeles approved all animal experimental protocols.

Plasma Creatine Kinase (CK) Activity Analysis

Plasma creatine kinase activity was determined using a colorimetric detection kit (Pointe Scientific Inc. Canto, MI) according to the manufacturer's instructions.

Histological Analysis of Skeletal Muscle

The whole muscle mass was dissected from the lower hindlimbs of mice, mounted onto a filter paper, and then snap-frozen in liquid nitrogen. The frozen cross-sections from midbelly of each muscle were stained with a battery of histochemical stains, including hematoxylin and eosin, Oil Red O, and NADH-tetrazolium reductase as previously described (Verity, 1991). Necrotic myofibers were scored in H&E stained sections as pale, swollen fibers that had evidence of breaks in the muscle fiber membrane (Haller and Drachman, 1980). To quantitate occurrence of necrotic fibers or central nucleated fibers, non-overlapping images of the transverse sections of were tiled together to provide an entire muscle cross–section, and fibers were counted on the entire muscle section using ImageJ (Liu et al., 2011). To plot the frequency distribution of fiber area, approximately 500 and 300 fibers randomly selected from cross-sections of tibialis anterior and soleus muscle, respectively, were analyzed with ImageJ (3 mice per group).

Lipid Analyses

Lipid analyses were performed as previously described (Zhang et al., 2012). Briefly, lipids were extracted from the lower hindlimb muscle of mice by a modification of the Bligh and

Dyer method. Phospholipid, sphingolipid, and diacylglycerol species were quantitated by electrospray ionization-tandem mass spectrometry. Triacylglycerol, free cholesterol, cholesteryl ester, and free fatty acid levels were determined using reagents from Wako (Richmond, VA). Phosphatidic acid (PA) in primary mouse embryonic fibroblasts (MEFs) or C2C12 myocytes was determined with a Total PA kit (Cayman, Ann Arbor, MI) (Zhang et al., 2012), and diacylgycerol (DAG) was assessed with a mouse DAG ELISA kit (MyBiosource Inc., San Diego, CA) (Cai and Sewer, 2013).

Muscle Oxygen Consumption Rate Measurements

Soleus muscle was isolated from mice and immediately finely minced in PBS, placed in the bottom of a Seahorse Islet Capture Microplate, and oxygen consumption was assessed with the Seahorse XF Extracellular Flux Analyzer (Seahorse Bioscience, Billerica, MA) as described previously (Vergnes et al., 2011).

Autophagy Analyses

Autophagic flux was assessed with the RFP-GFP-LC3 reporter plasmid (ptfLC3) as described (Kimura et al., 2007). Primary MEFs cells split in a 12-well plate were infected with lipin-1 adenoviruses for 16h, then transfected with ptfLC3 using BioT transfection reagent (Bioland Scientific LLC, Paramount CA). Images were acquired with a confocal laser scanning microscope (Leica SP2 1P-FCS; Bensheim, Germany). Puncta structures with GFP–RFP and/or RFP signals were quantified in more than 80 cells per group, and the degree of autophagosome maturation was expressed as percent of puncta with red color.

Endogenous Lipin-1, LC3, and LAMP-1 Immunohistochemistry

For co-localization of lipin-1 and LAMP-1, 4-d post-differentiation C2C12 myotubes were treated with 2μM rapamycin (Sigma Aldrich, St Louis, MO) for 8h, 10μM lovastatin (Sigma Aldrich) for 16h, or DMSO as control. Immunostaining was performed with as described (Peterson et al., 2011). For co-localization of LC3 with LAMP-1, primary MEFs cells infected with lipin-1 adenoviruses for 16h, then transfected for 24 h, and starved with Hank's Balanced Salt Solution (HBSS) for 3 h. Sources of the antibodies: anti-lipin-1 was a kind gift of Dr. Thurl Harris (Harris et al., 2007), anti-LC3 antibody was from Novus Biologicals, and rat anti-LAMP-1 antibody was from BD Pharmingen (San Jose, CA). Images were acquired by confocal laser scanning microscopy.

Vps34 Activity and PtIns3P production Assay

Vps34 activity was detected by visualization of phosphatidylinositol 3-phosphate (PtIns3P) production on autophagosomes or autolysosomes using the $p40^{phox}$-EGFP reporter (Kanai et al., 2001). Primary MEFs were co-transfected with mRFP-LC3 and $p40^{phox}$-EGFP plasmids and subcultured onto collagen-coated coverslips. After overnight incubation, coverslips were washed and culture medium replaced with Hank's Balanced Salt Solution (HBSS) for 6 h. Puncta appearing yellow represent autophagosomes or autolysosomes containing PtIns3P, whereas puncta appearing red represent autophagosomes or autolysosomes without PtIns3P. The percentage of phagosomes containing PtIns3P was determined as the proportion of yellow puncta to total puncta from 80 cells of each group.

Statistical Analyses

The results are shown as mean ± S.D. We performed two-way analysis of variance (ANOVA), or one-way ANOVA, followed with Bonferroni correction for multiple comparisons (Stata 11). A p value < 0.05 was considered statistically significant.

Supplementary Material

Refer to Web version on PubMed Central for supplementary material.

Acknowledgments

We gratefully acknowledge Dr. Tamotsu Yoshimori for the gift of GFP-LC3, mRFP-LC3, and mRFP-GFP-LC3 plasmids, Dr. Michael B. Yaffe for the gift of $p40^{phox}$-EGFP reporter plasmids, and Dr. Thurl Harris for anti-lipin-1 antibody. We thank Dr. Laurent Vergnes for advice on mitochondrial function studies, Qin Han for mouse embryonic fibroblast preparation, and Ping Xu for mouse genotyping and technical assistance. This work was supported by the National Institutes of Health P01 HL028481 (KR). The Seahorse XF24 instrument was supported by a shared instrument grant from the NIH NCRR (S10RR026744). Lipidomic analyses by mass spectrometry were performed at the Kansas Lipidomics Research Center Analytical Laboratory, which was supported by National Science Foundation grants EPS 0236913, MCB 0455318 and 0920663, and DBI 0521587, NIH P20RR16475, Kansas State University, the Kansas Technology Enterprise Corp., and K-IDeA Networks of Biomedical Research Excellence.

REFERENCES

Asp L, Kartberg F, Fernandez-Rodriguez J, Smedh M, Elsner M, Laporte F, Barcena M, Jansen KA, Valentijn JA, Koster AJ, Bergeron JJ, Nilsson T. Early stages of Golgi vesicle and tubule formation require diacylglycerol. Molecular biology of the cell. 2009; 20:780–790. [PubMed: 19037109]

Baron CL, Malhotra V. Role of diacylglycerol in PKD recruitment to the TGN and protein transport to the plasma membrane. Science (New York, N.Y. 2002; 295:325–328.

Bergounioux J, Brassier A, Rambaud C, Bustarret O, Michot C, Hubert L, Arnoux JB, Lazquerriere A, Bekri S, Galene-Gromez S, Bonnet D, Hubert P, de Lonlay P. Fatal rhadomyolysis in 2 children with LPIN1 mutations. J. Pediatr. 2012; 160:1052–1054. [PubMed: 22480698]

Cai K, Sewer MB. cAMP-stimulated transcription of DGKtheta requires steroidogenic factor 1 and sterol regulatory element binding protein 1. J Lipid Res. 2013; 54:2121–2132. [PubMed: 23610160]

Chargé SBP, Rudnicki MA. Cellular and molecular regulation of muscle regeneration. Physiol. Rev. 2004; 84:209–238. [PubMed: 14715915]

Ching JK, Elizabeth SV, Ju JS, Lusk C, Pittman SK, Weihl CC. mTOR dysfunction contributes to vacuolar pathology and weakness in valosin-containing protein associated inclusion body myopathy. Human molecular genetics. 2013; 22:1167–1179. [PubMed: 23250913]

Cho K, Hill MM, Chigurupati S, Du G, Parton RG, Hancock JF. Therapeutic levels of the hydroxymethylglutaryl-coenzyme A reductase inhibitor Lovastatin activate Ras signaling via phospholipase D2. Mol. Cell Biol. 2011; 31:1110–1120. [PubMed: 21245384]

Csaki LS, Dwyer JR, GFong LG, Tontonoz P, Young SG, Reue K. Lipins, lipinopathies, and the modulation of cellular lipid storage and signaling. Prog. Lipid Res. 2013; 52:305–316. [PubMed: 23603613]

Donkor J, Sariahmetoglu M, Dewald J, Brindley DN, Reue K. Three mammalian lipins act as phosphatidate phosphatases with distinct tissue expression patterns. The Journal of biological chemistry. 2007; 282:3450–3457. [PubMed: 17158099]

Eaton JM, Mullins GR, Brindley DN, Harris TE. Phosphorylation of lipin 1 and charge on the phosphatidic acid head group control its phosphatidic acid phosphatase activity and membrane association. J. Biol. Chem. 2013; 288:9933–9945. [PubMed: 23426360]

Eisenberg-Lerner A, Kimchi A. PKD is a kinase of Vps34 that mediates ROS-induced autophagy downstream of DAPk. Cell death and differentiation. 2012; 19:788–797. [PubMed: 22095288]

Ellwanger K, Kienzle C, Lutz S, Jin ZG, Wiekowski MT, Pfizenmaier K, Hausser A. Protein kinase D controls voluntary-running-induced skeletal muscle remodelling. The Biochemical journal. 2011; 440:327–324. [PubMed: 21848513]

Fernandez-Ulibarri I, Vilella M, Lazaro-Dieguez F, Sarri E, Martinez SE, Jimenez N, Claro E, Merida I, Burger KN, Egea G. Diacylglycerol is required for the formation of COPI vesicles in the Golgi-to-ER transport pathway. Molecular biology of the cell. 2007; 18:3250–3263. [PubMed: 17567948]

Finck BN, Gropler MC, Chen Z, Leone TC, Croce MA, Harris TE, Lawrence JC Jr. Kelly DP. Lipin 1 is an inducible amplifier of the hepatic PGC-1alpha/PPARalpha regulatory pathway. Cell Metab. 2006; 4:199–210. [PubMed: 16950137]

Germain M, Nguyen AP, Le Grand JN, Arbour N, Vanderluit JL, Opferman JT, Slack RS. MCL-1 is a stress sensor that regulates autophagy in a develomentally regulated manner. EMBO J. 2011; 30:395–407. [PubMed: 21139567]

Haller RG, Drachman DB. Alcoholic rhabdomyolysis: an experimental model in the rat. Science (New York, N.Y.). 1980; 208:412–415.

Han GS, Wu WI, Carman GM. The Saccharomyces cerevisiae Lipin homolog is a Mg2+-dependent phosphatidate phosphatase enzyme. The Journal of biological chemistry. 2006; 281:9210–9218. [PubMed: 16467296]

Hanai J, Cao P, Tanksale P, Imamura S, Koshimizu E, Zhao J, Kishi S, Yamashita M, Phillips PS, Sukhatme VP, Lecker SH. The muscle-specific ubiquitin ligase atrogin-1/MAFbx mediates statin-induced muscle toxicity. The Journal of clinical investigation. 2007; 117:3940–3951. [PubMed: 17992259]

Harris TE, Huffman TA, Chi A, Shabanowitz J, Hunt DF, Kumar A, Lawrence JC Jr. Insulin controls subcellular localization and multisite phosphorylation of the phosphatidic acid phosphatase, lipin 1. The Journal of biological chemistry. 2007; 282:277–286. [PubMed: 17105729]

He C, Bassik MC, Moresi V, Sun K, Wei Y, Zou Z, An Z, Loh J, Fisher J, Sun Q, Korsmeyer S, Packer M, May HI, Hill JA, Virgin HW, Gilpin C, Xiao G, Bassel-Duby R, Scherer PE, Levine B. Exercise-induced BCL2-regulated autophagy is required for muscle glucose homeostasis. Nature. 2012; 481:511–515. [PubMed: 22258505]

Huffman TA, Mothe-Satney I, Lawrence JC Jr. Insulin-stimulated phoephorylation of lipin mediated by the mammalian target of rapamycin. Proc. Natl. Acad. Sci. USA. 2002; 99:1047–1052. [PubMed: 11792863]

Huynh KK, Eskelinen E-L, Malevanets A, Saftig P, Grinstein S. LAMP proteins are required for fusion of lysosomes with phagosomes. EMBO J. 2007; 26:313–324. [PubMed: 17245426]

Jaber N, Dou Z, Chen JS, Catanzaro J, Jiang YP, Ballou LM, Selinger E, Ouyang X, Lin RZ, Zhang J, Zong WX. Class III PI3K Vps34 plays an essential role in autophagy and in heart and liver function. Proceedings of the National Academy of Sciences of the United States of America. 2012; 109:2003–2008. [PubMed: 22308354]

Jensen TE, Maarbjerg SJ, Rose AJ, Leitges M, Richter EA. Knockout of the predominant conventional PKC isoform, PKCalpha, in mouse skeletal muscle does not affect contraction-stimulated glucose uptake. American journal of physiology. 2009; 297:E340–348. [PubMed: 19458061]

Kabeya Y, Mizushima N, Ueno T, Yamamoto A, Kirisako T, Noda T, Kominami E, Ohsumi Y, Yoshimori T. LC3, a mammalian homologue of yeast Apg8p, is localized in autophagosome membranes after processing. Embo J. 2000; 19:5720–5728. [PubMed: 11060023]

Kanai F, Liu H, Field SJ, Akbary H, Matsuo T, Brown GE, Cantley LC, Yaffe MB. The PX domains of p47phox and p40phox bind to lipid products of PI(3)K. Nature cell biology. 2001; 3:675–678.

Kim HB, Kumar A, Wang L, Liu GH, Keller SR, Lawrence JC Jr. Finck BN, Harris TE. Lipin 1 represses NFATc4 transcriptional activity in adipocytes to inhibit secretion of inflammatory factors. Mol Cell Biol. 2010; 30:3126–3139. [PubMed: 20385772]

Kimura S, Noda T, Yoshimori T. Dissection of the autophagosome maturation process by a novel reporter protein, tandem fluorescent-tagged LC3. Autophagy. 2007; 3:452–460. [PubMed: 17534139]

Las G, Serada SB, Wikstrom JD, Twig G, Shirihai OS. Fatty acids suppress autophagic turnover in beta-cells. The Journal of biological chemistry. 2011; 286:42534–42544. [PubMed: 21859708]

Levine B, Kroemer G. Autophagy in the pathogenesis of disease. Cell. 2008; 132:27–42. [PubMed: 18191218]

Liang C, Lee J-S, Inn K-S, Gack MU, Li Q, Roberts EA, Vergne I, Deretic V, Feng P, Akazawa C, Jung JU. Beclin1-binding UVRAG targets the class C Vps complex to coordinate autophagosome maturation and endocytic trafficking. Nature cell biology. 2008; 10:776–787.

Link E, Parish S, Armitage J, Bowman L, Heath S, Matsuda F, Gut I, Lathrop M, Collins R. SLCO1B1 variants and statin-induced myopathy--a genomewide study. The New England journal of medicine. 2008; 359:789–799. [PubMed: 18650507]

Liu N, Bezprozvannaya S, Shelton JM, Frisard MI, Hulver MW, McMillan RP, Wu Y, Voelker KA, Grange RW, Richardson JA, Bassel-Duby R, Olson EN. Mice lacking microRNA 133a develop dynamin 2-dependent centronuclear myopathy. The Journal of clinical investigation. 2011; 121:3258–3268. [PubMed: 21737882]

Mangravite LM, Engelhardt BE, Medina MW, Smith JD, Brown CD, Chasman DI, Mecham BH, Howie B, Shim H, Naidoo D, Feng Q, Rieder MJ, Chen YD, Rotter JI, Ridker PM, Hopewell JC, Parish S, Armitage J, Collins R, Wilke RA, Nickerson DA, Stephens M, Krauss RM. A statin-dependent QTL for GATM expression is associated with statin-induced myopathy. Nature. 2013; 502:377–380. [PubMed: 23995691]

Michot C, Hubert L, Brivet M, De Meirleir L, Valayannopoulos V, Muller-Felber W, Venkateswaran R, Ogier H, Desguerre I, Altuzarra C, Thompson E, Smitka M, Huebner A, Husson M, Horvath R, Chinnery P, Vaz FM, Munnich A, Elpeleg O, Delahodde A, de Keyzer Y, de Lonlay P. LPIN1 gene mutations: a major cause of severe rhabdomyolysis in early childhood. Hum Mutat. 2010; 31:E1564–1573. [PubMed: 20583302]

Michot C, Hubert L, Romero NB, Gouda A, Mamoune A, Mathew S, Kirk E, Viollet L, Rahman S, Bekri S, Peters H, McGill J, Glamuzina E, Farrar M, von der Hagen M, Alexander IE, Kirmse B, Barth M, Laforet P, Benlian P, Munnich A, Jeanpierre M, Elpeleg O, Pines O, Delahodde A, de Keyzer Y, de Lonlay P. Study of LPIN1, LPIN2 and LPIN3 in rhabdomyolysis and exercise-induced myalgia. J Inherit Metab Dis. 2012; 35:1119–1128. [PubMed: 22481384]

Michot C, Mamoune A, Vamecq J, Viou MT, Hsieh LS, Testet E, Laine J, Hubert L, Dessein AF, Fontaine M, Ottolenghi C, Fouillen L, Nadra K, Blanc E, Bastin J, Candon S, Pende M, Munnich A, Smahi A, Djouadi F, Carman GM, Romero N, de Keyzer Y, de Lonlay P. Combination of lipid metabolism alterations and their sensitivity to inflammatory cytokines in human lipin-1-deficient myoblasts. Biochimica et biophysica acta. 2013; 1832:2103–2114. [PubMed: 23928362]

Mizushima N, Yoshimori T, Levine B. Methods in mammalian autophagy research. Cell. 2010; 140:313–326. [PubMed: 20144757]

Mohassel P, Ammane AL. The spectrum of statin myopathy. Curr. Opin. Rheumatol. 2013; 25:747–752. [PubMed: 24061077]

Needham M, Mastaglia FL. Statin myotoxicity: A review of genetic susceptibility factors. Neuromuscul Disord. 2013

Pascual F, Carman GM. Phosphatidate phosphatase, a key regulator of lipid homeostasis. Biochimica et biophysica acta. 2013; 1831:514–522. [PubMed: 22910056]

Pascual F, Hsieh LS, Soto-Cardalda AI, Carman GM. Yeast Pah1p phosphatidate phosphatase is regulated by proteasome-mediated degradation. J. Biol. Chem. Epub ahead of print. 2014

Peterfy M, Phan J, Xu P, Reue K. Lipodystrophy in the fld mouse results from mutation of a new gene encoding a nuclear protein, lipin. Nat Genet. 2001; 27:121–124. [PubMed: 11138012]

Peterson TR, Sengupta SS, Harris TE, Carmack AE, Kang SA, Balderas E, Guertin DA, Madden KL, Carpenter AE, Finck BN, Sabatini DM. mTOR Complex 1 Regulates Lipin 1 Localization to Control the SREBP Pathway. Cell. 2011; 146:408–420. [PubMed: 21816276]

Phan J, Reue K. Lipin, a lipodystrophy and obesity gene. Cell Metab. 2005; 1:73–83. [PubMed: 16054046]

Phillips PS, Haas RH, Bannykh S, Hathaway S, Gray NL, Kimura BJ, Vladutiu GD, England JD. Statin-associated myopathy with normal creatine kinase levels. Ann Intern Med. 2002; 137:581–585. [PubMed: 12353945]

Shahnazari S, Yen WL, Birmingham CL, Shiu J, Namolovan A, Zheng YT, Nakayama K, Klionsky DJ, Brumell JH. A diacylglycerol-dependent signaling pathway contributes to regulation of antibacterial autophagy. Cell host & microbe. 2010; 8:137–146. [PubMed: 20674539]

Shibasaki M, Kurokawa K, Katsura M, Ohkuma S. Direct evidence for the up-regulation of Vps34 regulated by PKCgamma during short-term treatment with morphine. Synapse (New York, N.Y. 2009; 63:365–368.

Storz P, Doppler H, Johannes FJ, Toker A. Tyrosine phosphorylation of protein kinase D in the pleckstrin homology domain leads to activation. The Journal of biological chemistry. 2003; 278:17969–17976. [PubMed: 12637538]

Sugden MC, Caton PW, Holness MJ. PPAR control: it's SIRTainly as easy as PGC. The Journal of endocrinology. 2010; 204:93–104. [PubMed: 19770177]

Tan SH, Shui G, Zhou J, Li JJ, Bay BH, Wenk MR, Shen HM. Induction of autophagy by palmitic acid via protein kinase C-mediated signaling pathway independent of mTOR (mammalian target of rapamycin). The Journal of biological chemistry. 2012; 287:14364–14376. [PubMed: 22408252]

Thompson PD, Clarkson P, Karas RH. Statin-associated myopathy. Jama. 2003; 289:1681–1690. [PubMed: 12672737]

Ugrankar R, Liu Y, Provaznik J, Schmitt S, Lehmann M. Lipin is a central regulator of adipose tissue development and function in Drosophila melanogaster. Mol Cell Biol. 2011; 31:1646–1656. [PubMed: 21300783]

Vergnes L, Chin R, Young SG, Reue K. Heart-type fatty acid-binding protein is essential for efficient brown adipose tissue fatty acid oxidation and cold tolerance. The Journal of biological chemistry. 2011; 286:380–390. [PubMed: 21044951]

Verity MA. Infantile Pompe's disease, lipid storage, and partial carnitine deficiency. Muscle & nerve. 1991; 14:435–440. [PubMed: 1870635]

Wang K, Klionsky DJ. Mitochondria removal by autophagy. Autophagy. 2011; 7:297–300. [PubMed: 21252623]

Yu L, McPhee CK, Zheng L, Mardones GA, Rong Y, Peng J, Mi N, Zhao Y, Liu Z, Wan F, Hailey DW, Oorschot V, Klumperman J, Baehrecke EH, Lenardo MJ. Termination of autophagy and reformation of lysosomes regulated by mTOR. Nature. 2010; 465:942–946. [PubMed: 20526321]

Zeharia A, Shaag A, Houtkooper RH, Hindi T, de Lonlay P, Erez G, Hubert L, Saada A, de Keyzer Y, Eshel G, Vaz FM, Pines O, Elpeleg O. Mutations in LPIN1 cause recurrent acute myoglobinuria in childhood. Am J Hum Genet. 2008; 83:489–494. [PubMed: 18817903]

Zhang P, Takeuchi K, Csaki LS, Reue K. Lipin-1 phosphatidic acid phosphatase activity modulates phosphatidate levels to promote peroxisome proliferator-activated receptor γ (PPARγ) gene expression during adipogenesis. J. Biol. Chem. 2012; 287:3485–3494. [PubMed: 22157014]

HIGHLIGHTS

- Lipin-1 deficiency causes muscle damage related to impaired autophagy clearance
- Lipin-1 phosphatidate phosphatase activity promotes autolysosome maturation
- Autophagy flux in lipin-1–deficient cells is rescued by activated protein kinase D
- Lipin-1 and statin drug effects converge in the autophagy pathway in muscle

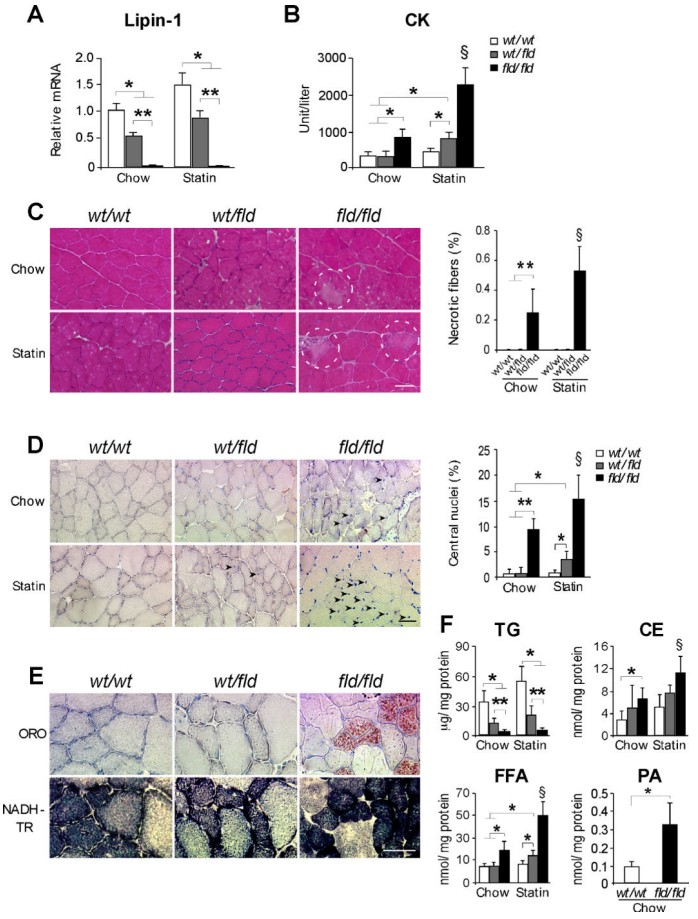

Figure 1. Myopathy in Lipin-1–deficient and Statin-treated Lipin-1–haploinsufficient Mice

(A) *Lpin1* mRNA levels in muscle of lipin-1–deficient (*fld/fld*), heterozygous (*wt/fld*), and wild type (*wt/wt*) mice (n = 6 mice/genotype).

(B) Plasma creatine kinase (CK) activity in mice fasted 16 h and refed for 5 h (n = 5-12 mice per group).

(C) *Left*, Representative image of necrotic myofibers (enclosed in dashed line circles) in transverse section of lower hindlimb muscle (H&E stain). *Right*, Necrotic myofiber frequency as a percentage of total fiber number (n = 5 mice per group). Scale bars in panels (C), (D) and (E) correspond to 50µm.

(D) *Left*, Representative image of centrally nucleated myofibers (arrowheads) in transverse section of lower hindlimb muscle (methyl Green stain). *Right*, Centrally nucleated myofiber frequency as a percentage of total fiber number (n = 5).

(E) *Upper*, Oil Red O (ORO)-stained sections from tibialis anterior muscle. *Lower*, NADH-tetrazolium reductase (NADH-TR) staining of sections adjacent to those stained with ORO. Lipid accumulation present in type I fibers (dark blue), but not type II fibers (light blue).

(F) Lipid quantification in lower hindlimb muscle from mice under basal and statin treated conditions. Measurements were made biochemically (TG, CE, FFA) or with electrospray ionization mass spectrometry (PA) (n = 3-6). TG, triacylglycerol; CE, cholesteryl esters, FFA, unesterified fatty acids; PA, phosphatidic acid. *, $p < 0.05$; **, $p < 0.01$ *vs.* indicated group; §, $p < 0.05$, *vs.* all other groups.

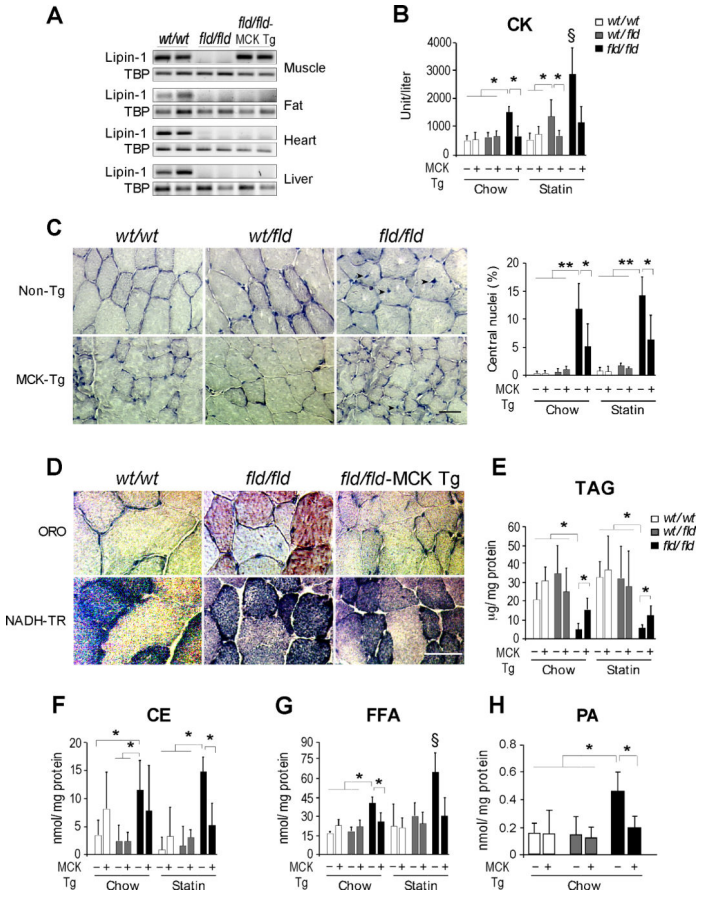

Figure 2. Muscle Lipin-1 Transgene Ameliorates Muscle Breakdown and Statin-Induced Myopathy

(A) RT-PCR analysis of *Lpin1* mRNA in tissues of wild-type (*wt/wt*), *fld/fld*, or *fld/fld* mice with MCK-lipin-1 transgene (*fld/fld*–MCK Tg).

(B) Muscle lipin-1 transgene normalizes plasma CK to wild-type levels in *fld/fld* mice and in *wt/fld* mice treated with statin (n = 3-6 mice per group).

(C) Muscle lipin-1 transgene reduces the frequency of centrally nucleated myofibers in *fld/fld* mice under basal conditions. *Left*, representative centrally nucleated myofibers (arrowheads) in transverse section of hindlimb muscle (Methyl Green stain). *Right*, frequency of centrally nucleated fibers as percentage of total fiber number (n = 3-6). Scale bars in panels (C) and (D) correspond to 50µm.

(D) Muscle lipin-1 transgene prevents the accumulation of neutral lipid droplets in skeletal muscle of *fld/fld* mice. Staining is as described in Figure 1E.

(E–H) Lipid levels in lower hindlimb muscle of *fld/fld*–MCK Tg and littermates of all genotypes, as indicated (n = 3-6). Lipid abbreviations as in Fig. 1F. *, $p < 0.05$; **, $p < 0.01$ *vs.* indicated groups; §, $p < 0.05$ *vs.* all other groups.

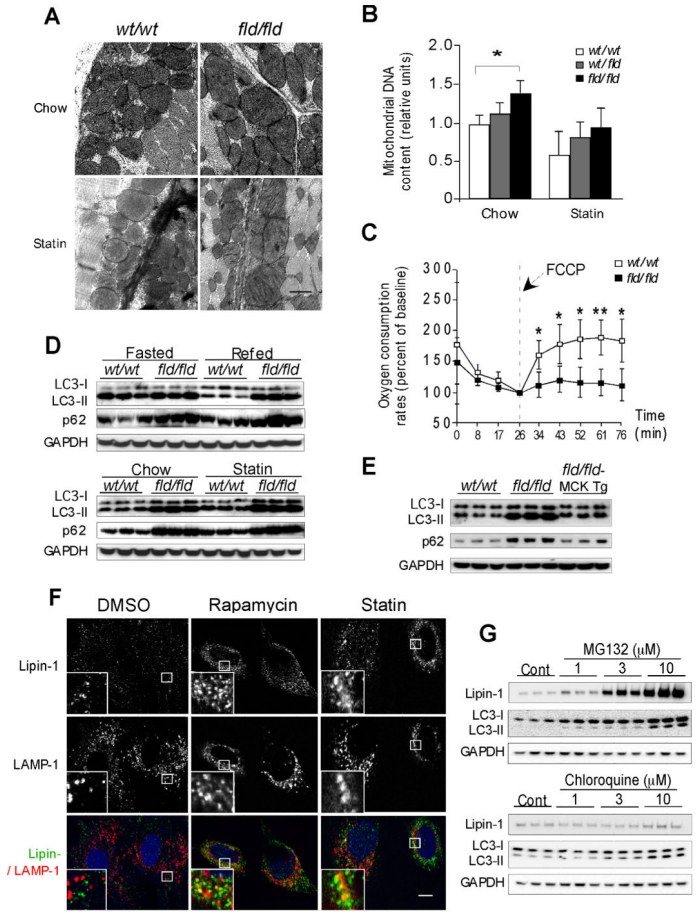

Figure 3. Lipin-1 Deficiency Impairs Mitochondrial Function and Autophagy Clearance in Muscle

(A) Representative electron micrographs showing accumulation of swollen, abnormally shaped mitochondria in *fld/fld* soleus muscle under the basal condition (*Upper*), and presence of disorganized cristae after statin treatment (*Lower*). Scale bar = 0.5μm.

(B) Relative mitochondrial DNA content in hindlimb muscle of mice normalized to genomic DNA (n = 5-6).

(C) Real-time analysis of oxygen consumption rate in soleus muscle under the basal condition and after addition of respiration uncoupler, FCCP (mesoxalonitrile 4-trifluoromethoxyphenylhydrazone) (n = 5 mice per group). *wt/wt vs fld/fld*, *, $p < 0.05$; **, $p < 0.01$.

(D) Immunoblot analysis of LC3-I, LC3-II, and p62 proteins in the lower hindlimb muscle. *Upper*, mice on a chow diet were fasted for 16 h (Fasted) or fasted 16 h and refed for 5 h (Refed), as indicated. *Lower*, analysis of mice maintained under basal conditions (Chow) or statin treatment (analyzed after fasting 16 h and feeding 5 h).

(E) The muscle lipin-1 transgene prevents the accumulation of LC3-I, LC3-II, and p62 proteins in lower hindlimb muscle of *fld/fld* (analyzed after fasting 16 h and feeding 5 h).

(F) Co-localization of endogenous lipin-1 (green) and LAMP-1 (red) in C2C12 myotubes visualized by confocal fluorescence microscopy. Cells were analyzed under control

conditions (DMSO), after induction of autophagy (2 μM rapamycin), or statin treatment (10 μM lovastatin). Scale bar = 10μm.

(G) Lipin-1 is degraded through the proteasome pathway. HEK 293 cells were transfected with plasmids encoding lipin-1 for 16 hr, then treated with vehicle control, MG132, or chloroquine for an additional 20 h at concentrations indicated, and indicated protein levels determined by Western blot.

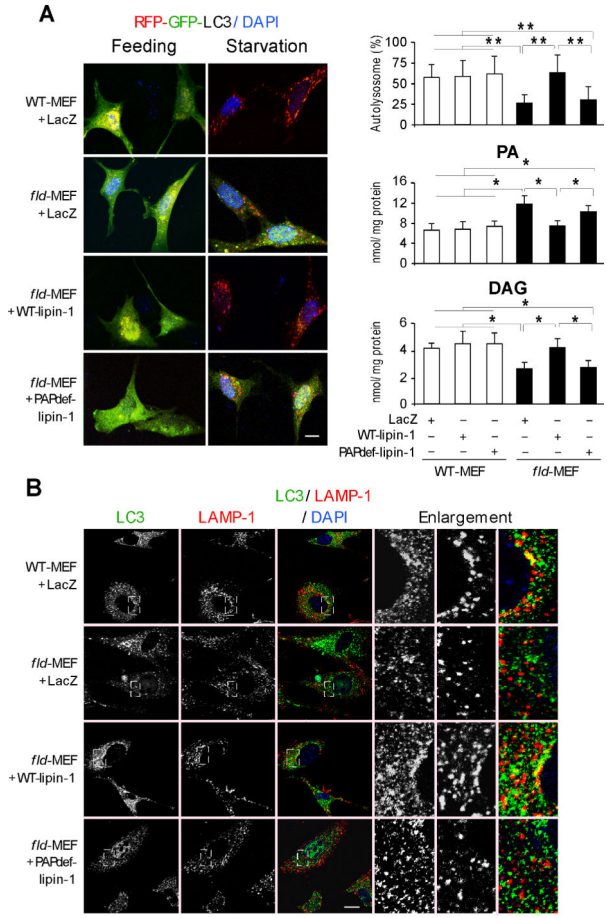

Figure 4. Lipin-1 PAP Activity is Required for Optimal Autolysosome Formation

(A) *Left*, autophagosome (yellow puncta) or autolysosome (red puncta) formation in mouse embryonic fibroblasts (MEFs) from wild-type (WT) and *fld/fld* mice infected with adenovirus expressing a control gene (LacZ), wild-type lipin-1 (WT-lipin-1), or PAP–deficient lipin-1 (PAPdef-lipin-1). Cells were depleted of glucose and amino acids for 6 hr. *Right*, quantification from experiments shown at left. Percentage of LC3 reporter present in autolysosomes (80 cells per group), and PA and diacylglycerol (DAG) level were determined biochemically (n=3). *, $p < 0.05$; **, $p < 0.01$.

(B) Co-localization by confocal microscopy of endogenous LC3 (green) and LAMP-1 (red) in primary MEFs infected with adenoviruses indicated at left. Enlargements from each of the panels are shown at right. Scale bars in panels (A) and (B) correspond to 10μm.

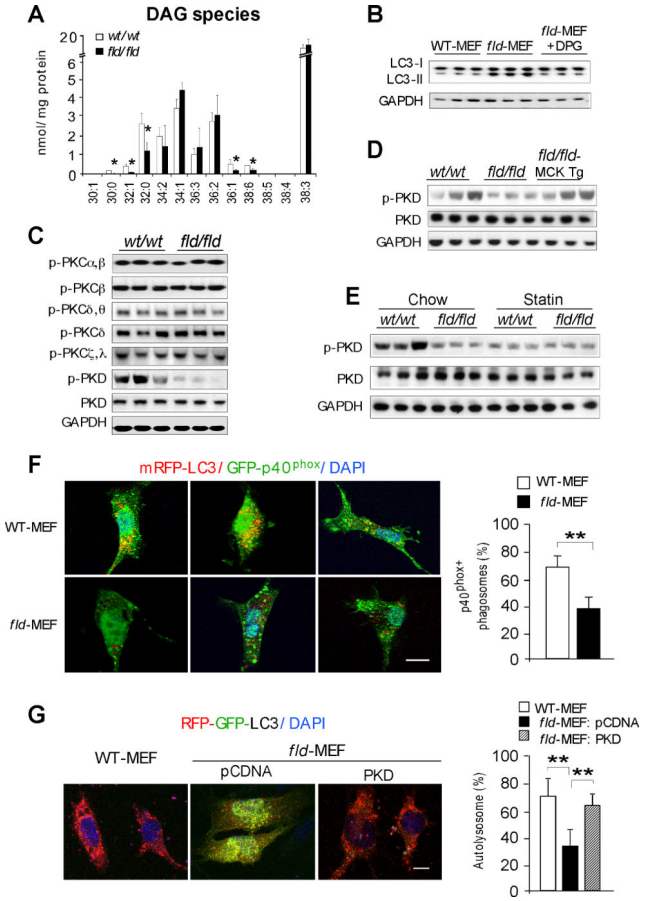

Figure 5. Lipin-1 Deficiency Inhibits the PKD-Vps34 Pathway in Autophagy Clearance

(A) Diacylglycerol quantification by electrospray ionization mass spectrometry in hindlimb muscle of wild-type (*wt/wt*) and *fld/fld* mice (n = 3). The molecular species of diacylglycerol in muscle are represented as the number of carbons:number of double bonds. *, $p < 0.05$.

(B) Immunoblot showing addition of 1,2-dipalmitoyl-sn-glycerol (DPG, 100 μM) increases LC3-II degradation in starved *fld*-MEFs.

(C) Immunoblot assessment of the activity of muscle protein kinase C (PKC) isoforms and protein kinase D (PKD) with the indicated antibodies.

(D) Muscle lipin-1 transgene rescues PKD activity in *fld/fld* muscle in mice under basal conditions.

(E) Immunoblot analysis of PKD activity in muscle of mice under basal (Chow) and statin treated conditions.

(F) Analysis of Vps34 activity in autophagy by co-localization of PtIns3P binding probe GFP-p40^{phox} and RFP-LC3 in primary MEFs after starvation. *Left*, representative confocal microscopy images, with PtIns3P presence in autophagosomes indicated by yellow puncta. *Right*, percentage of autophagosomes with visible yellow puncta, indicating presence of PtIns3P. n = 80 cells per group. Scale bars in panels (F) and (G) correspond to 10μm.

(G) Expression of active PKD restores autophagy flux in *fld*-MEFs. Constitutively active PKD (S738E/742E) and RFP-GFP-LC3 reporter were co-transfected into primary MEFs. *Left*, representative confocal microscopy images. Red puncta indicate formation of

autolysosomes. *Right*, percentage of LC3 reporter present in autolysosomes. n = 80 cells per group. *, $p < 0.05$.

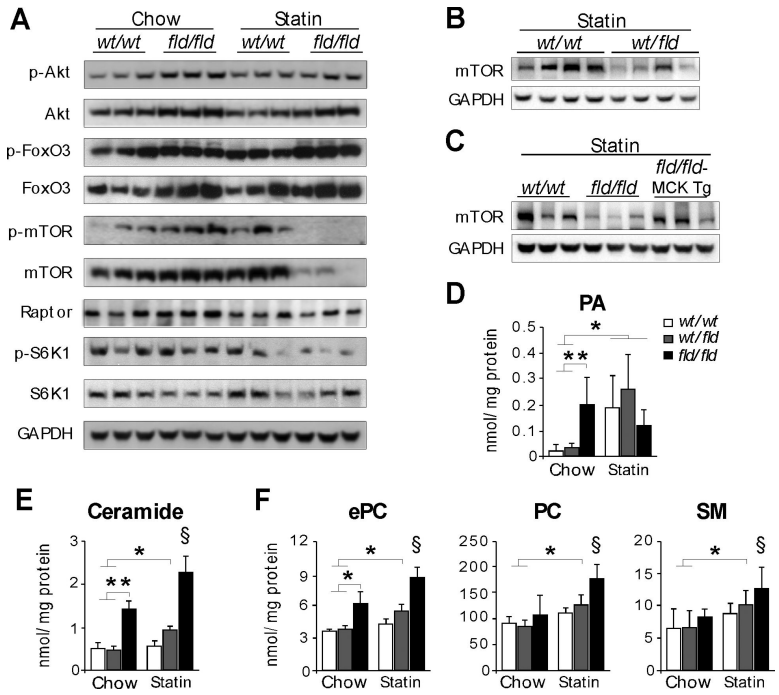

Figure 6. Statin Reduces mTOR Abundance and Promotes Lipid Accumulation in Lipin-1–deficient and –haploinsufficient Muscle

(A) Immunoblot assessment of Akt/FoxO3 and mTOR pathways in skeletal muscle using the indicated antibodies.

(B) Statin-induced reduction in mTOR levels of lipin-1-haploinsufficient (*wt/fld*) muscle.

(C) Muscle-specific lipin-1 transgene prevents statin-induced reduction in mTOR abundance in *fld/fld* muscle.

(D-F) Mass spectrometry analysis of phospholipids and sphingolipids in hindlimb muscle from mice under basal conditions and after statin treatment (n = 3–6). PA, phosphatidic acid; ePC, ether phosphatidylcholine; PC, phosphatidylcholine; SM, sphingomyelin. *, $p < 0.05$; **, $p < 0.01$ *vs.* indicated groups; §, $p < 0.05$ *vs.* all other groups.

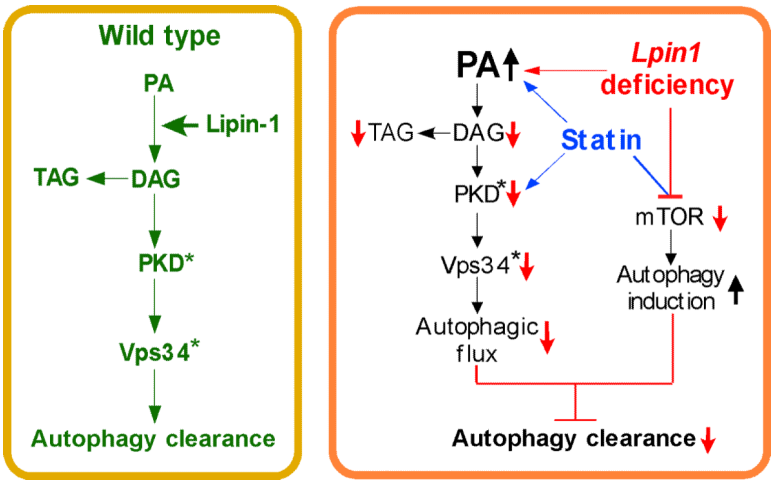

Figure 7. Proposed Role of Lipin-1 in Regulation of Lipid Levels, Autophagy Clearance, and Protection Against Statin Myotoxicity

Left, In wild-type muscle, lipin-1 converts PA to DAG, providing substrate for TAG synthesis and activating PKD, with subsequent activation of Vps34 during autolysosome assembly. These steps allow normal autophagy flux. *Right*, In lipin-1 deficiency (red arrows and lines), the lipin-1 enzyme substrate, PA, accumulates and DAG levels are reduced. This causes impaired TAG synthesis, reduced PKD/Vps34 activation (active forms signified by asterisk), and reduced autophagic flux. Statin treatment has similar effects as lipin-1 deficiency at some points (blue arrows and lines). Statins cause increased PA accumulation and reduced PKD activation both in wild-type and lipin-1–haploinsufficient backgrounds. In addition, statin treatment in combination with lipin-1-haploinsufficiency or lipin-1 deficiency causes reduced mTOR activation, and autophagy initiation. The net result of statin treatment and reduced lipin-1 activity is to increase autophagy initiation, but prevent optimal flux through the pathway, leading to impaired autophagy clearance.